# Electron Theory of Permanent Magnets

Takashi Miyake
(AIST, Tsukuba)

Elements Strategy Initiative Center for Magnetic Materials

# Outline

- Coercivity and magnetocrystalline anisotropy
- Rare-earth magnets
- Standard theory
- An example: $NdFe_{11}TiN$
- Interface and magnetic reversal

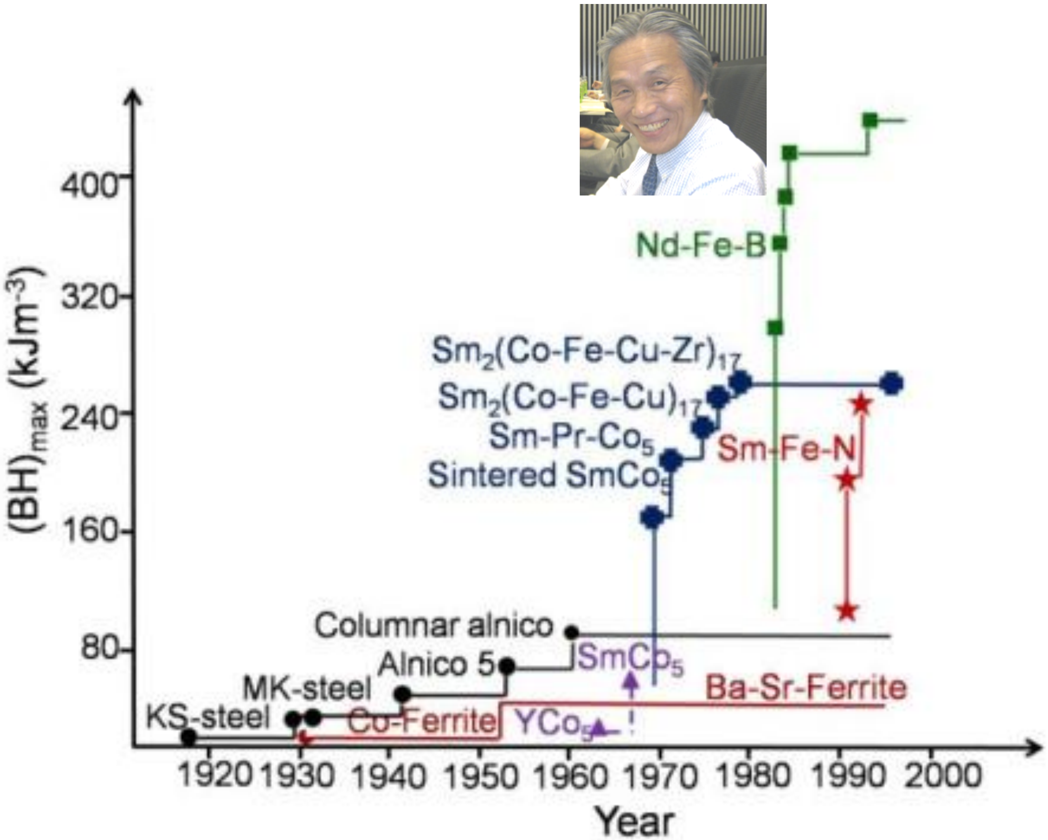


## $Nd_2Fe_{14}B$

$\mu_0 M_s$=1.61 T, $\mu_0 H_c$>0.8 T

$K_u$=4.3 MJ/m$^3$, $\kappa$=1.54

$(BH)_{max}$<510 kJ/m$^3$

$T_c$=312°C

Nd-Fe-B Ferrite

# Maximum energy product $(BH)_{max}$

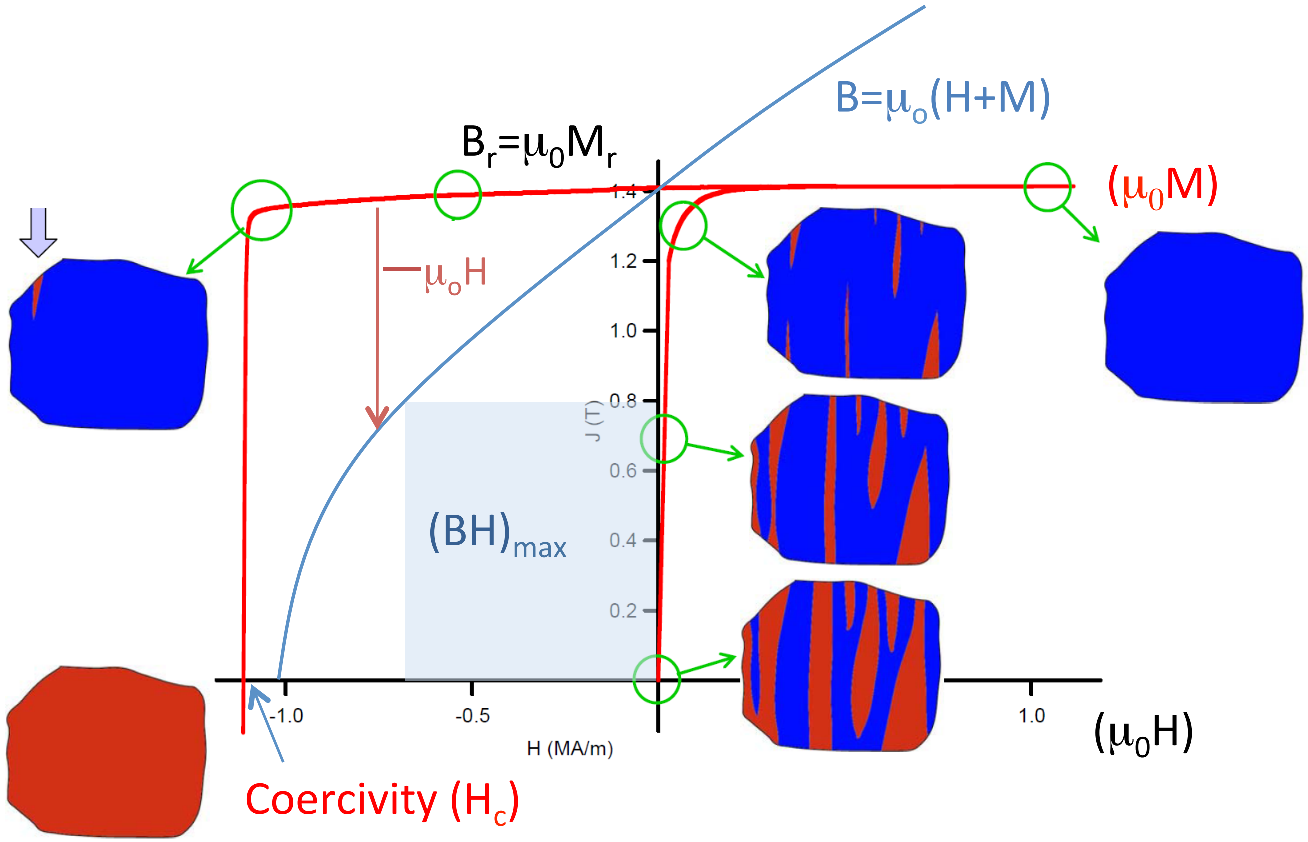

# Conditions for strong magnets

- Squareness
- Magnetization
- Coercivity

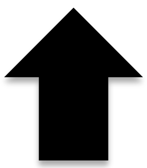

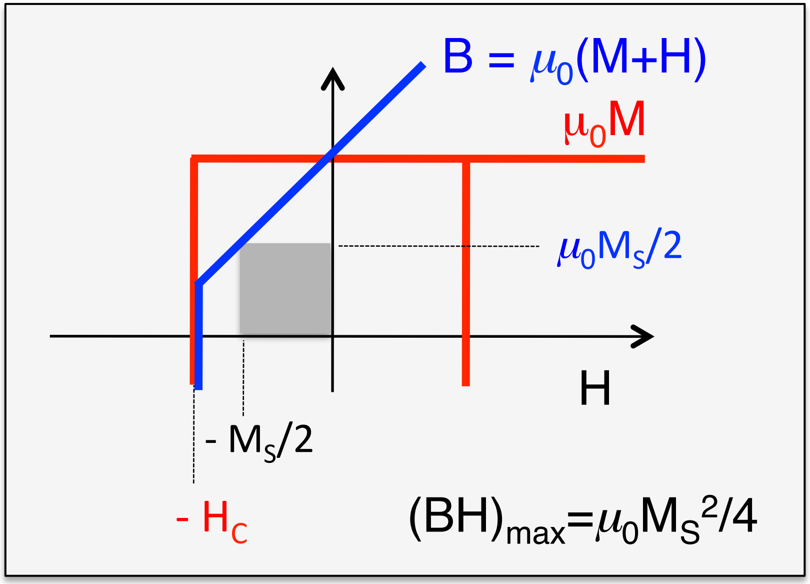


without using rare-metals
Temperature effects

$$(BH)_{max} = \mu_0 M_S^2/4 \quad \text{if} \quad H_C > M_S/2$$

# Anisotropy magnetic field

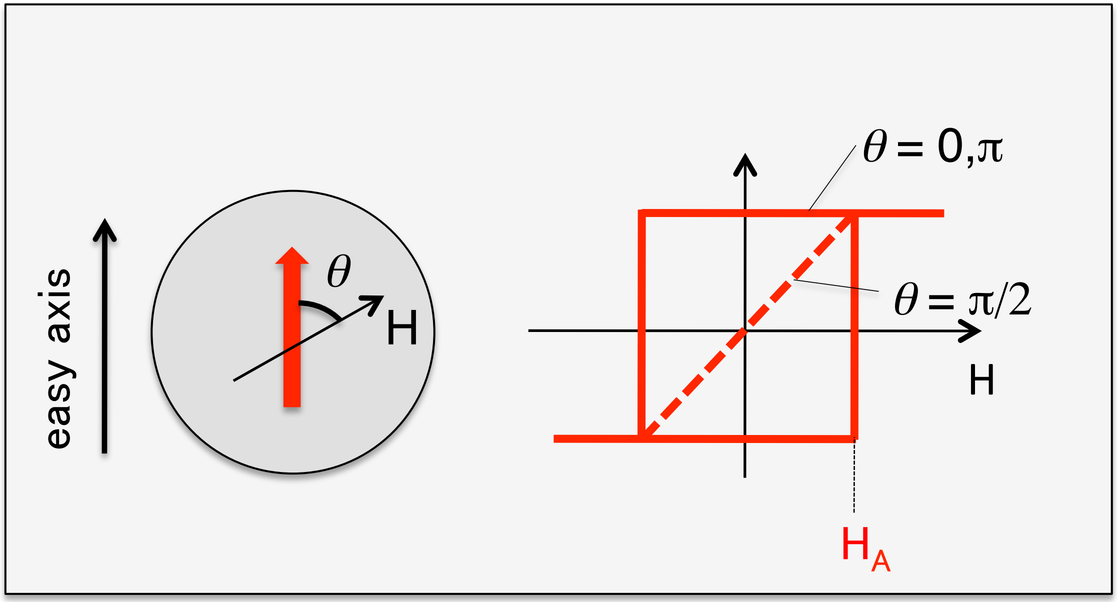


$Nd_2Fe_{14}B$

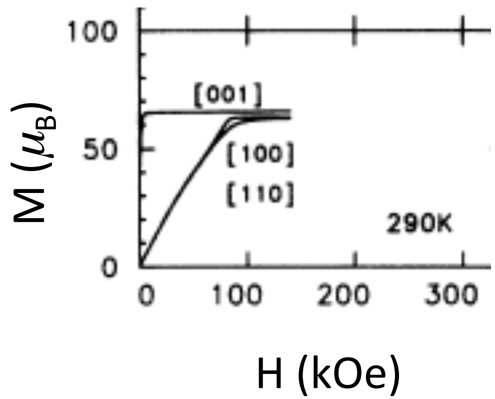


M. Yamada et al., PRB **38**, 620 (1988)

In the Stoner–Wolfarth model,

$$H_A = 2\, K_1 / (\mu_0 M_S)$$

$$E_A = K_1 \sin^2\theta + \cdots$$

Anisotropy magnetic field

Magnetic Anisotropy Energy

- Shape anisotropy
- Crystalline anisotropy

# Coercivity vs. anisotropy magnetic field

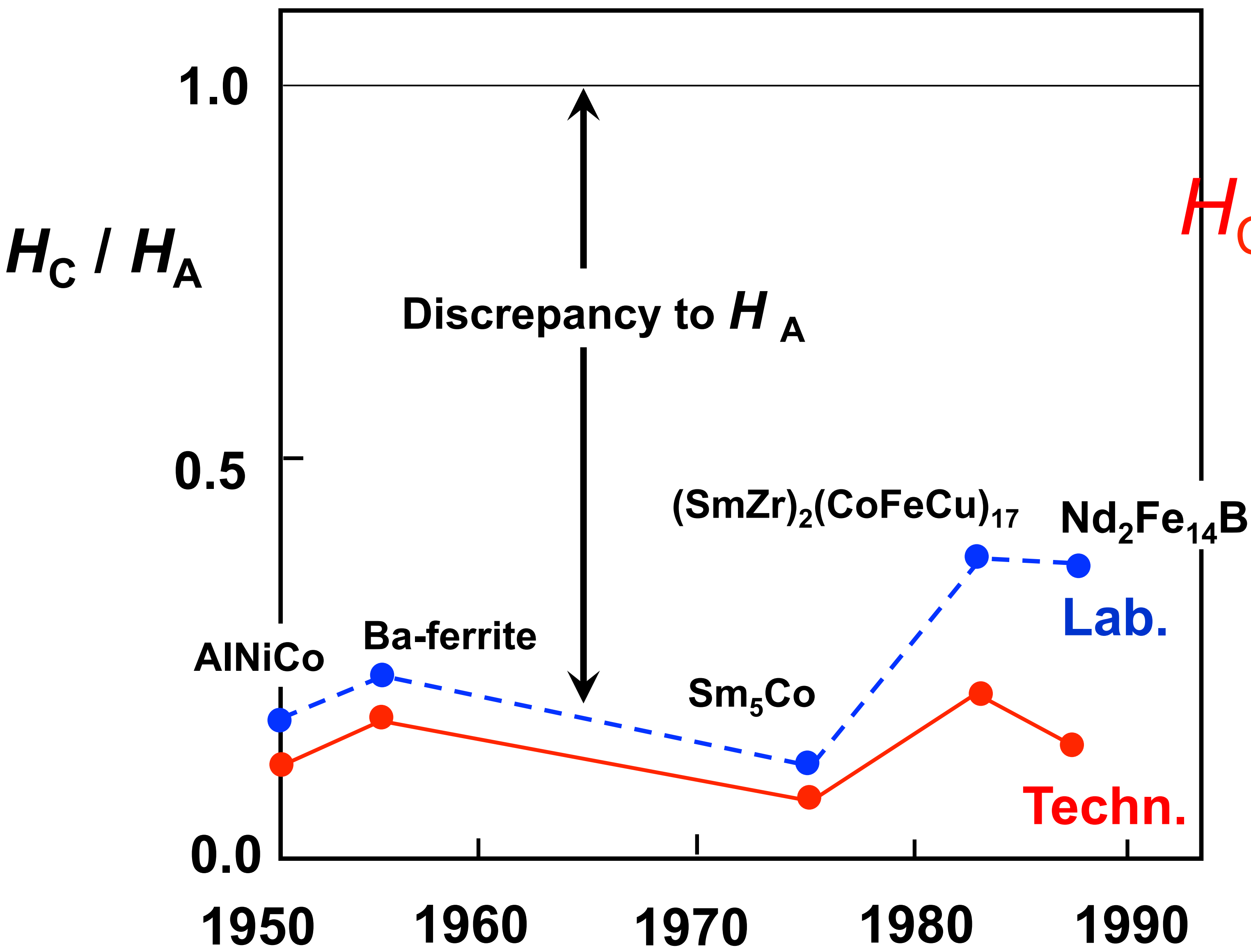


$H_C \propto H_A$
$\propto K$

# Dysprosium substitution

$(NdDy)_2Fe_{14}B$

- Rare-metal
- $(BH)_{max}$ smaller

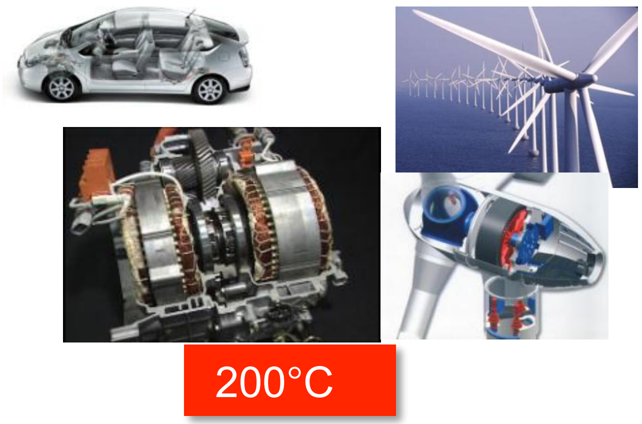


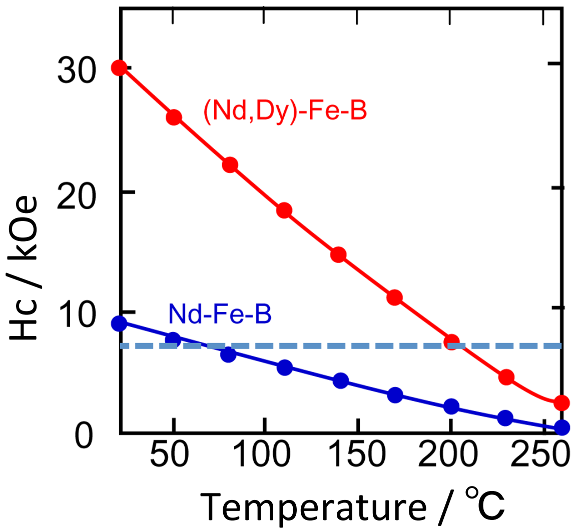


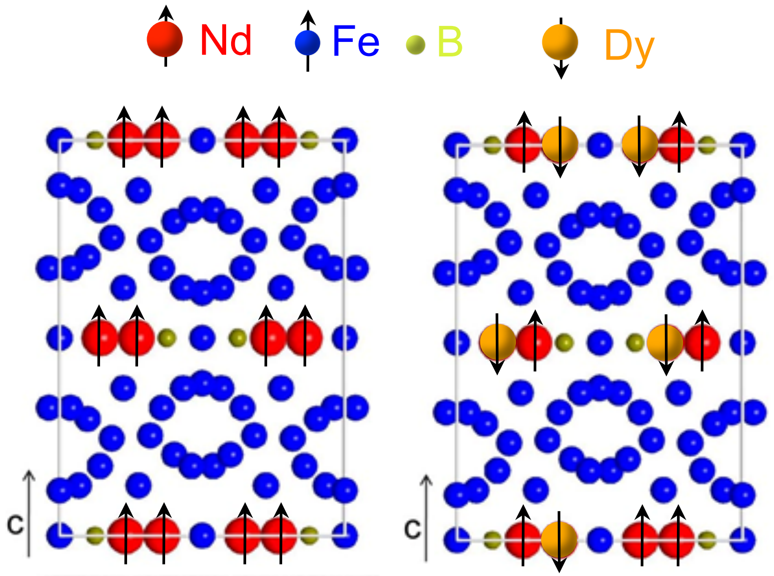


$\mathcal{K}(Nd_2Fe_{14}B) < \mathcal{K}(Dy_2Fe_{14}B)$

# Challenges

- Temperature dependence
  - MagnetoCrystalline Anisotropy (MCA) energy
  - Magnetization and Curie temperature
- Difference between coercivity and anisotropy magnetic field
- New hard magnets

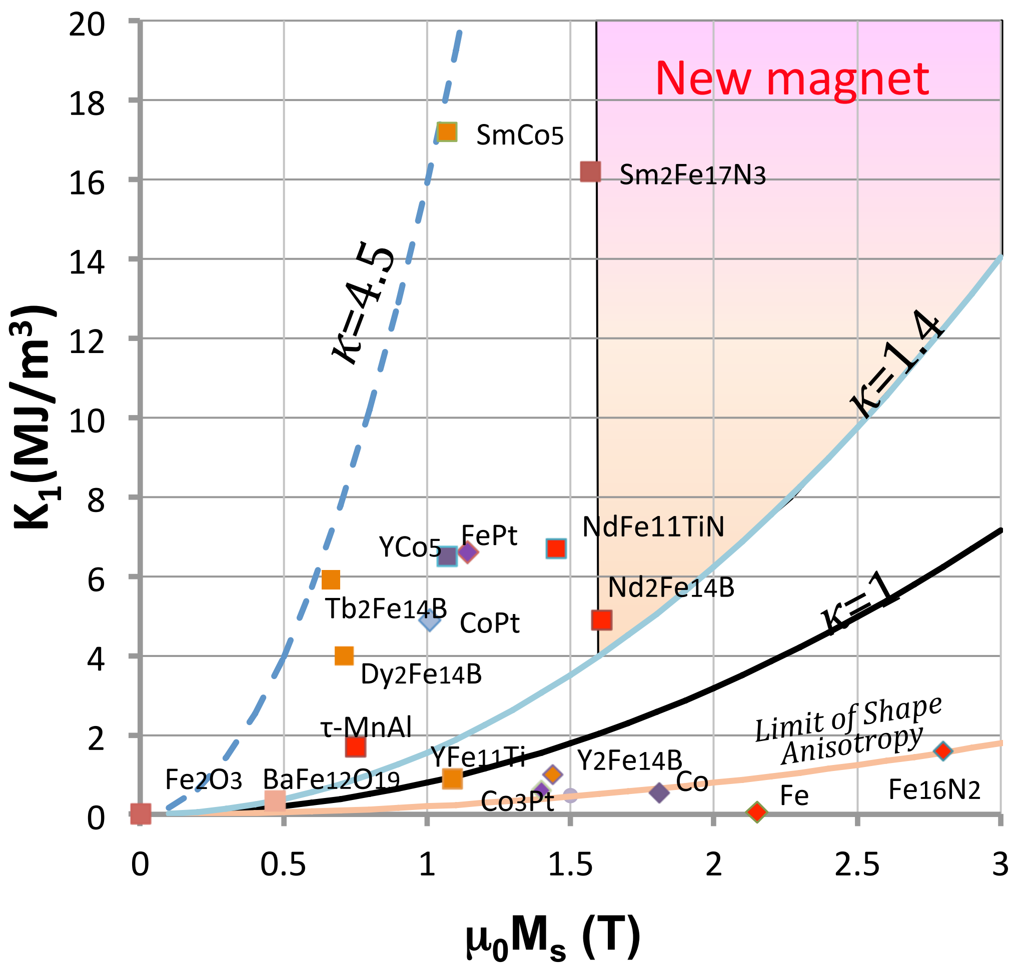


$$E_A = K_1 \sin^2\theta + \cdots$$

# Transition-metal alloys

$L1_0$-type alloy

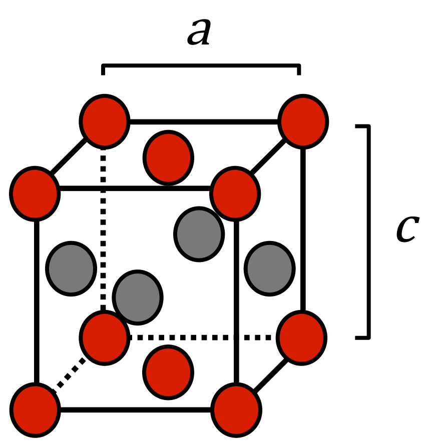


Fe (bcc): ~1 $\mu$eV
Co (hcp): ~60 $\mu$eV

FePt: ~3 meV/f.u.
CoPt: ~1 meV/f.u.

# Rare-earth magnets

| | $M_S$(T) | $K_1$(MJ/m$^3$) | $H_A$(MA/m) | $T_C$(K) | |
|---|---|---|---|---|---|
| $Nd_2Fe_{14}B$ | 1.60 | 4.5 | 5.3 | 586 | 2-14-1 family |
| $Pr_2Fe_{14}B$ | 1.56 | 5.5 | 6.9 | 569 | |
| $Dy_2Fe_{14}B$ | 0.712 | 5.4 | 11.9 | 598 | |
| $SmCo_5$ | 1.07 | 17.2 | 28 | 1,000 | 1-5 family |
| $Sm_2Co_{17}$ | 1.25 | 3.2 | 5.1 | 1,193 | 2-17 family |
| $Sm_2Fe_{17}N_3$ | 1.54 | 8.6 | 20.7 | 746 | |
| $NdFe_{11}TiN$ | 1.45 | 6.7 | 9.6 | 729 | 1-12 family |

# $Nd_2Fe_{14}B$

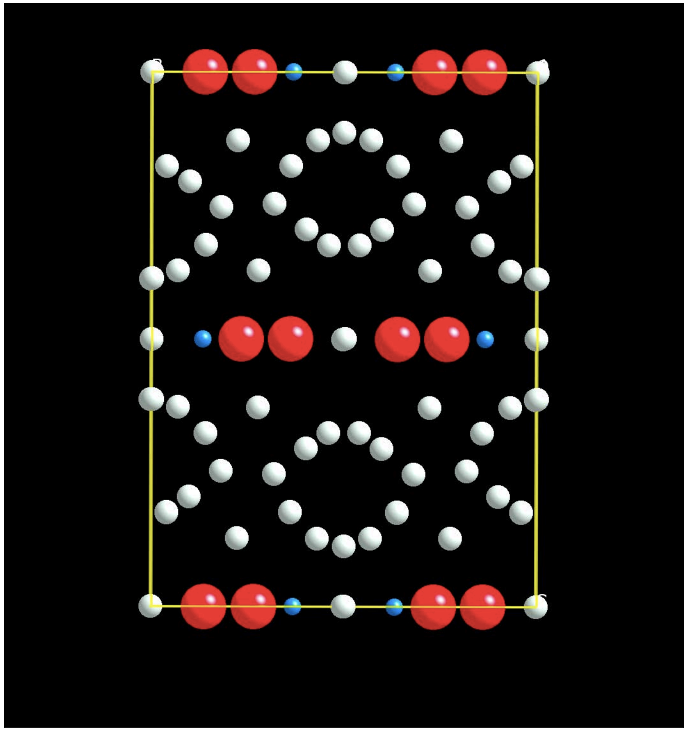

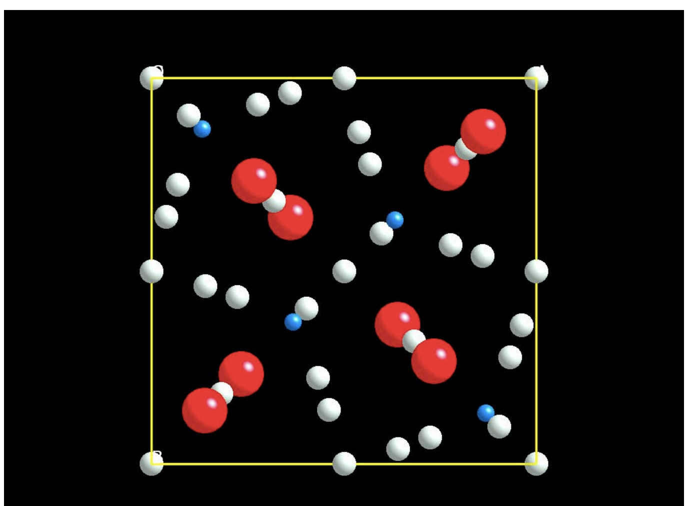

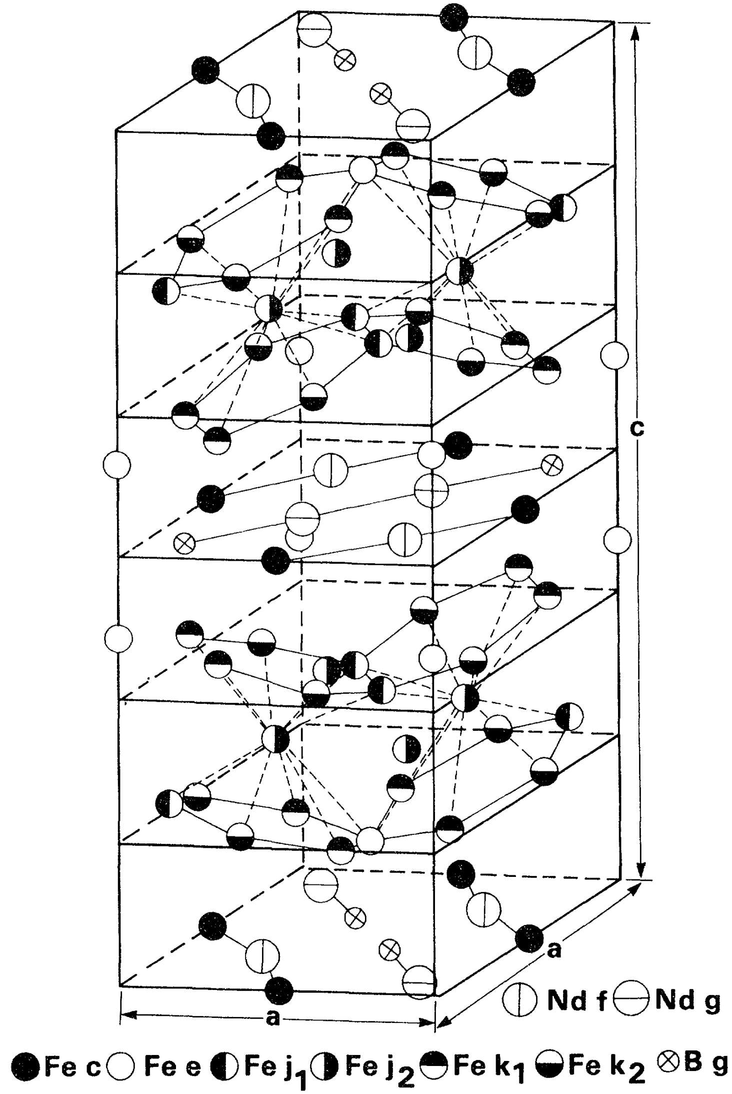


Herbst, RMP (1991)

# $R_{n-m}T_{5n+2m}$ series

n=1, m=0: 1-5 family (CaCu$_5$-type)
n=2, m=1: 1-12 family (ThMn$_{12}$-type)
n=3, m=1: 2-17 family (Th$_2$Zn$_{17}$-type, Th$_2$Ni$_{17}$-type)

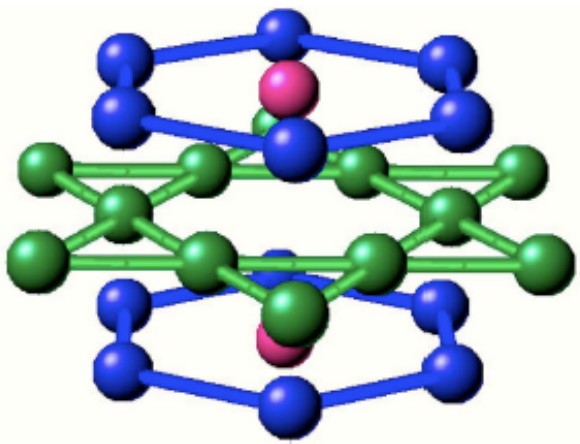

Larson, Mazin and Papaconstantopoulos, PRB 67, 214405 (2003)

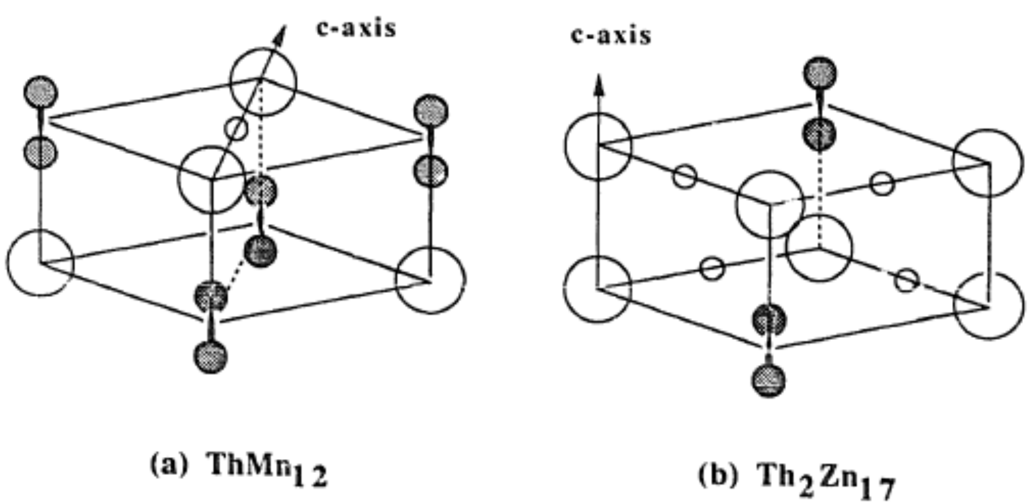


Li and Cadogan, JMMM 109, 153 (1992)

# Outline

- Coercivity and magnetocrystalline anisotropy
- Rare-earth magnets
- Standard theory
- An example: $NdFe_{11}TiN$
- Interface and magnetic reversal

# LDA band structure of $GdCo_5$

majority spin

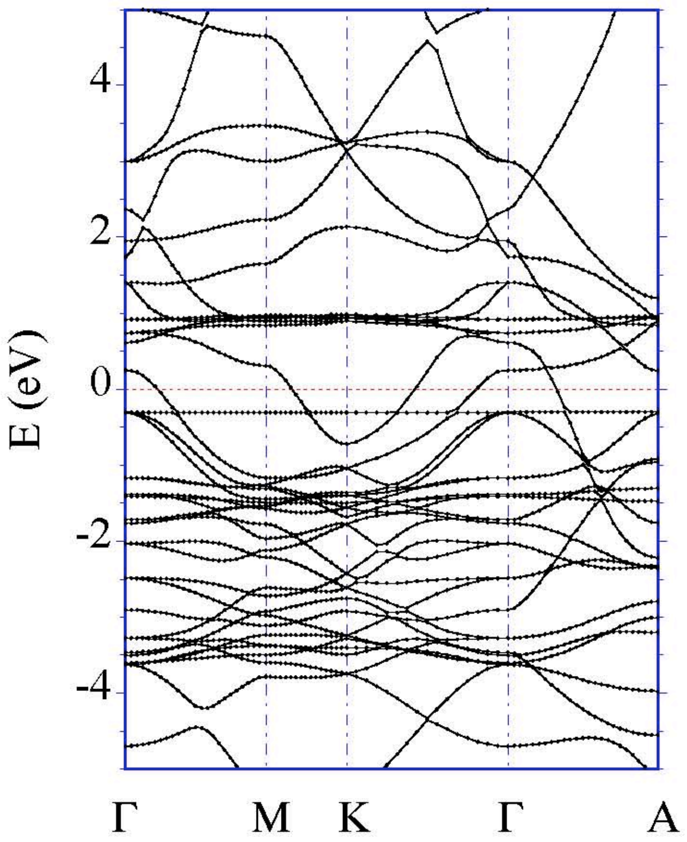


minority spin

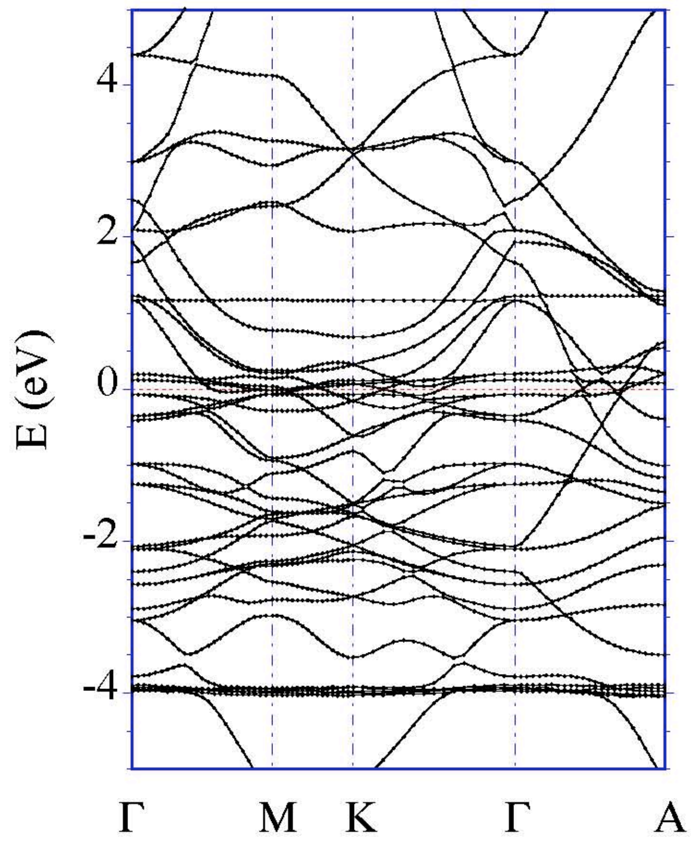

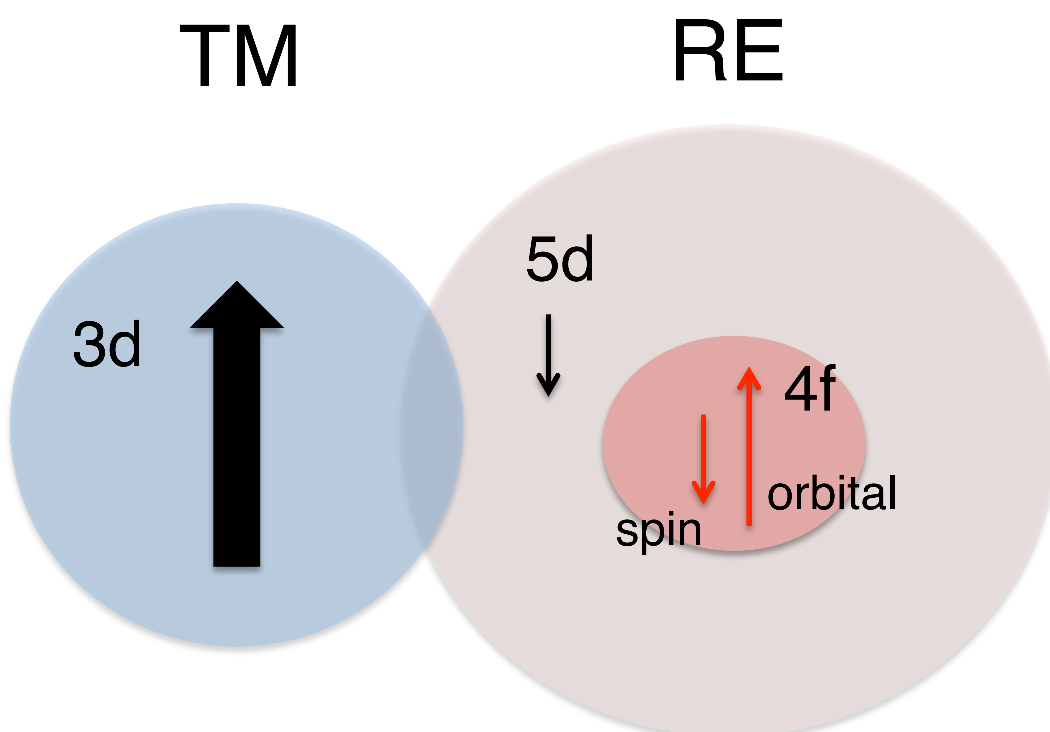


- large magnetization
- exchange coupling
  → Curie temp.

- strong SOC + crystal-electric field
  → MCA

# Effective Hamiltonian

$$H = \underline{2\boldsymbol{H}_{ex} \cdot \boldsymbol{S}} + \lambda \boldsymbol{L} \cdot \boldsymbol{S} + V_{cry}$$

Exchange magnetic field

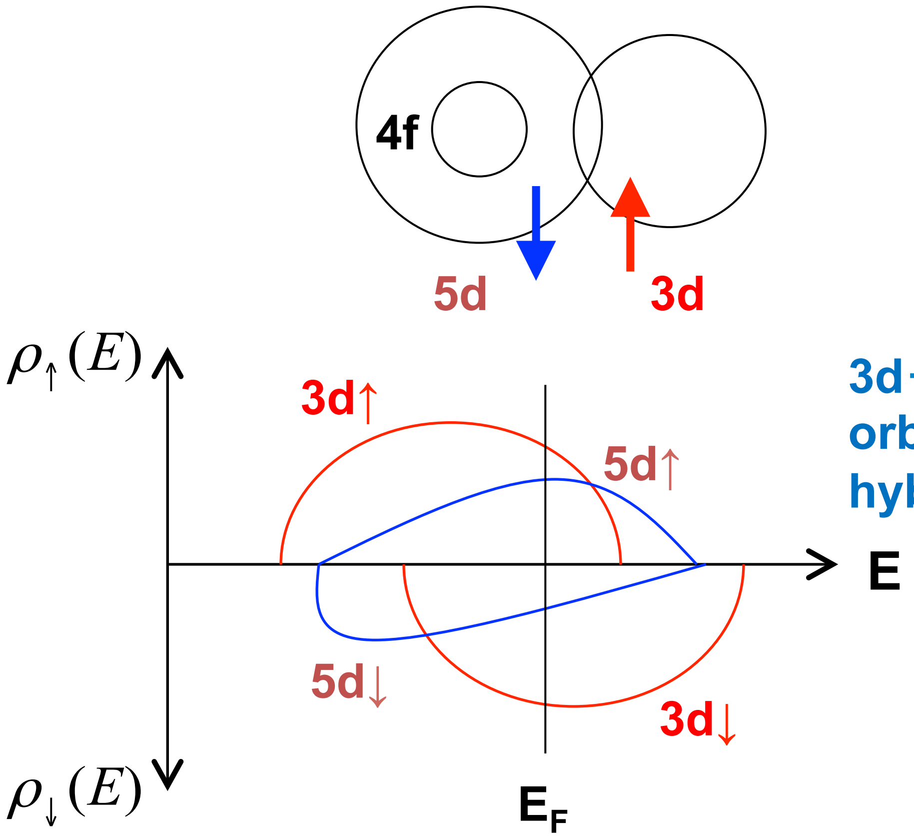


3d—5d orbital hybridization ⇨ spin anti-parallel

A. Sakuma

# Effective Hamiltonian

$$H = 2\boldsymbol{H}_{ex} \cdot \boldsymbol{S} + \lambda \boldsymbol{L} \cdot \boldsymbol{S} + V_{cry}$$

Exchange magnetic field

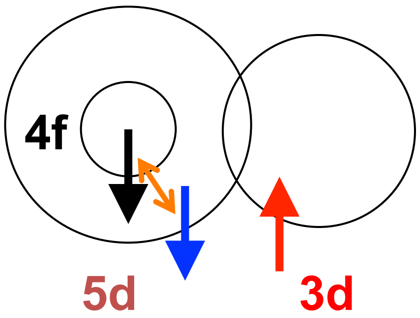


5d spin－4f spin

Hund coupling ⇨ spin parallel

A. Sakuma

# Effective Hamiltonian

$$H = 2\boldsymbol{H}_{ex} \cdot \boldsymbol{S} + \lambda \boldsymbol{L} \cdot \boldsymbol{S} + V_{cry}$$

Exchange magnetic field

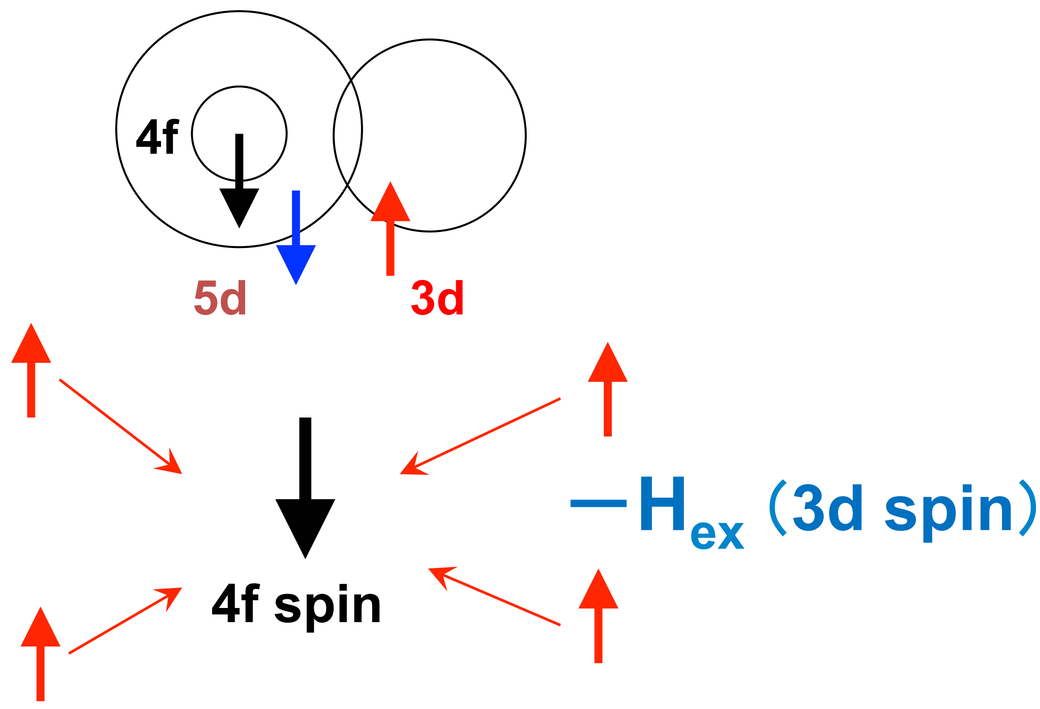


A. Sakuma

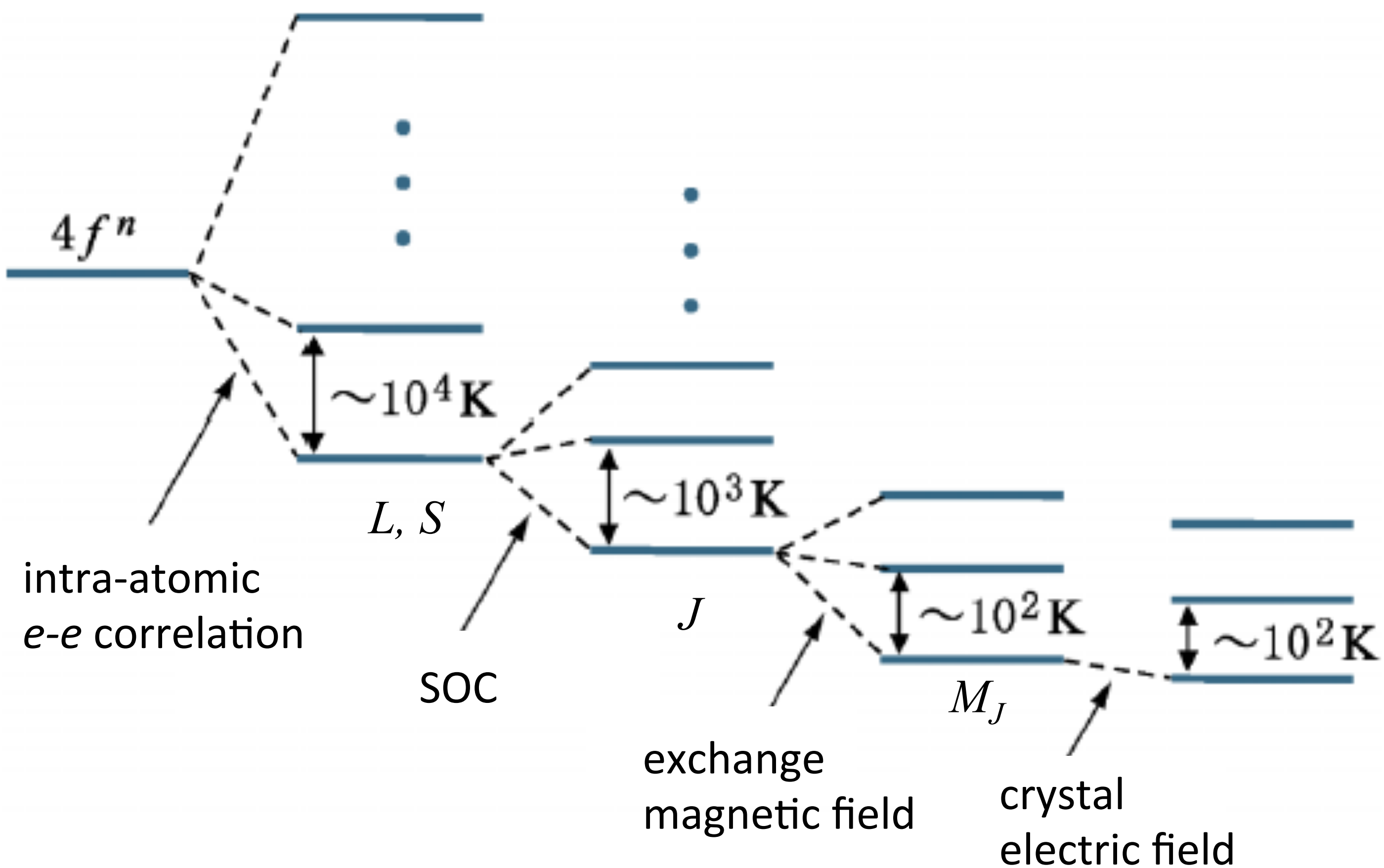

$4f^n$
$\sim 10^4$ K
$L, S$
$\sim 10^3$ K
$J$
$\sim 10^2$ K
$M_J$
$\sim 10^2$ K
intra-atomic
*e-e* correlation
SOC
exchange
magnetic field
crystal
electric field

# Effective Hamiltonian

$$H = 2\boldsymbol{H}_{ex} \cdot \boldsymbol{S} + \underline{\lambda \boldsymbol{L} \cdot \boldsymbol{S}} + V_{cry}$$

Spin-orbit interaction

**light rare-earth （n＜7）：** $\lambda > 0$ ⇨ ↑ + ↓ = ↑ *J* // − *S*

*L* *S* *J*＝|L－S|

**heavy rare-earth （n＞7）：** $\lambda < 0$ ⇨ ↑ + ↑ = ↑ *J* // *S*

*L* *S* *J*＝|L＋S|

**Gd（n＝7）：** $\lambda = 0$ ⇨ ↑ = ↑ *J* = *S*

*J*＝|S|

A. Sakuma

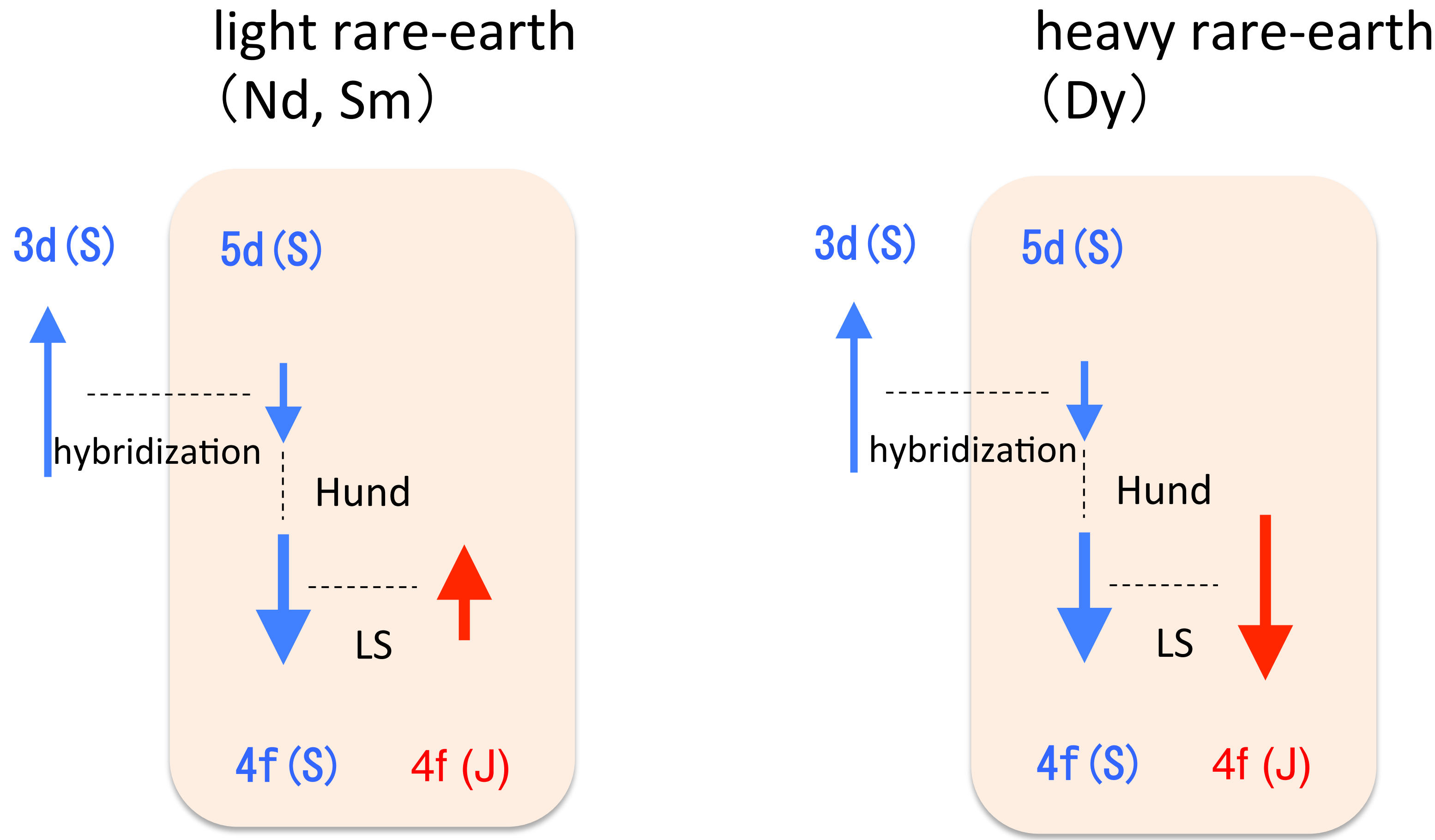
light rare-earth
(Nd, Sm)
heavy rare-earth
(Dy)
3d (S)
5d (S)
hybridization
Hund
LS
4f (S)
4f (J)
3d (S)
5d (S)
hybridization
Hund
LS
4f (S)
4f (J)

# Effective Hamiltonian

$$H = \underline{2\boldsymbol{H}_{ex} \cdot \boldsymbol{S} + \lambda \boldsymbol{L} \cdot \boldsymbol{S}} + V_{cry}$$

$$\Downarrow$$

$$2(g_J - 1)\boldsymbol{J} \cdot \boldsymbol{H}_{ex}$$

$$g_J = 1 + \frac{J(J+1) + S(S+1) - L(L+1)}{2J(J+1)}$$ **Lande factor**

light RE： $J = |L - S|$ ⇨ $g_J < 1$

heavy RE： $J = |L + S|$ ⇨ $g_J > 1$

A. Sakuma

# Effective Hamiltonian

$$H = 2\boldsymbol{H}_{ex} \cdot \boldsymbol{S} + \lambda \boldsymbol{L} \cdot \boldsymbol{S} + \underline{V_{cry}}$$

**Crystal Electric Field (CEF)**

$$V_{cry} = \sum_i V_{cry}(\boldsymbol{r}_i)$$

$$= \sum_i \sum_j \frac{-|e|q_j}{|\boldsymbol{r}_i - \boldsymbol{R}_j|}$$

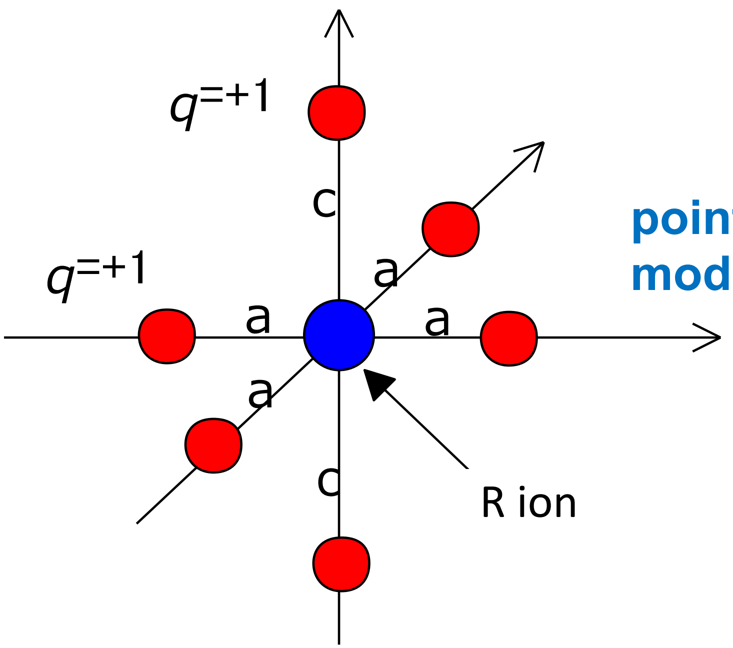


**point charge model**

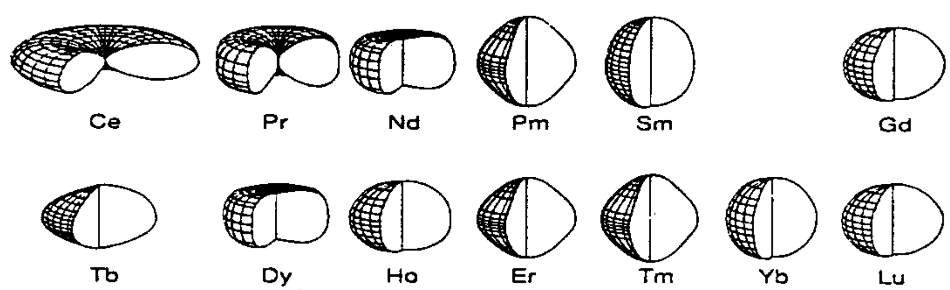


A. Sakuma

# Effective Hamiltonian

$$H = 2\boldsymbol{H}_{ex} \cdot \boldsymbol{S} + \lambda \boldsymbol{L} \cdot \boldsymbol{S} + V_{cry}$$

**Crystal Electric Field (CEF)**

$$V_{cry} = \sum_i V_{cry}(\boldsymbol{r}_i)$$

$$= \sum_i \sum_j \frac{-|e| q_j}{|\boldsymbol{r}_i - \boldsymbol{R}_j|}$$

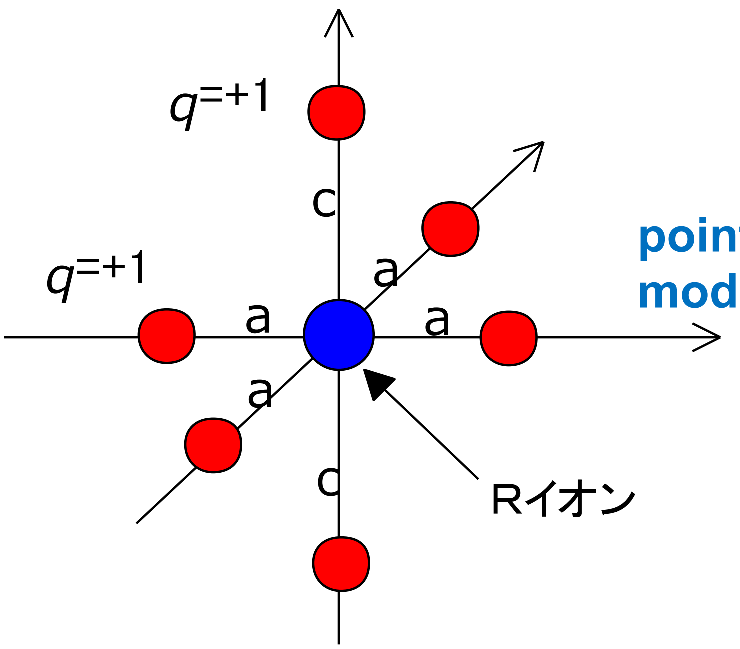


**point charge model**

$$\Rightarrow \sum_i \sum_{l,m} r_i^l A_l^m Q_l^m(x_i, y_i, z_i)$$

**Spherical Harmonics**

A. Sakuma

# Stevens' operator-equivalent method

$$H = 2(g_J - 1)\boldsymbol{J} \cdot \boldsymbol{H}_{ex} + \sum_{l,m} B_l^m O_l^m$$

$$B_l^m = \theta_J < r^l > A_l^m$$

$$\theta_2 = \alpha_J,\ \theta_4 = \beta_J,\ \theta_6 = \gamma_J$$

$$< r^l > = \int dr\, f_{l=3}(r)\, r^l\, f_{l=3}(r)$$

Stevens' factor

$A_l^m$ CEF parameter

$$O_2^0 = 3J_z^2 - J(J+1)$$

$$O_2^2 = J_x^2 - J_y^2$$

$$O_2^{-2} = (J_+^2 - J_-^2)/2$$

$$O_4^4 = (J_+^4 + J_-^4)/2$$

MCA energy

$$K_1 = -3J(J - 1/2)\,\alpha_J \langle r^2 \rangle A_2^0$$

A. Sakuma

$$K_1 = -3J(J-1/2)\alpha_J\langle r^2\rangle A_2^0$$

Depend on *R* ion

CEF surrounding the *R* ion

4f electrons

CEF

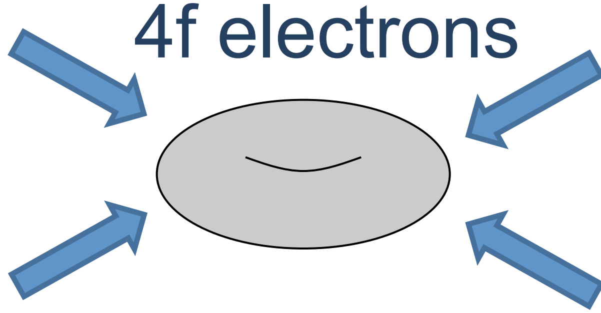

$A_2^0$

**CEF parameter**

$J$

$\alpha_J$

$\langle r^2\rangle$

A. Sakuma

$$K_1 = -3J(J-1/2)\alpha_J \langle r^2 \rangle A_2^0$$

| | $\alpha_J \times 10^2$ | $J$ |
|---|---|---|
| Nd | -0.64 | 9/2 |
| Dy | -0.63 | 15/2 |
| Sm | +4.13 | 5/2 |

opposite sign

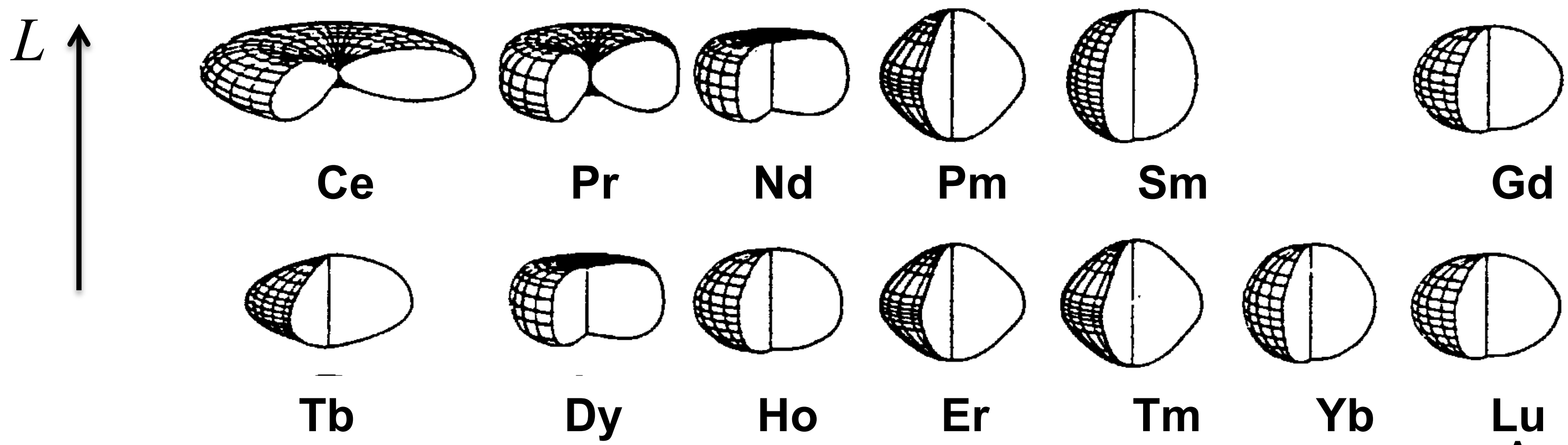


A. Sakuma

$$K_1 = -3J(J-1/2)\alpha_J \langle r^2 \rangle A_2^0$$

| | $\alpha_J \times 10^2$ | $J$ |
|---|---|---|
| Nd | -0.64 | 9/2 |
| Dy | -0.63 | 15/2 |
| Sm | +4.13 | 5/2 |

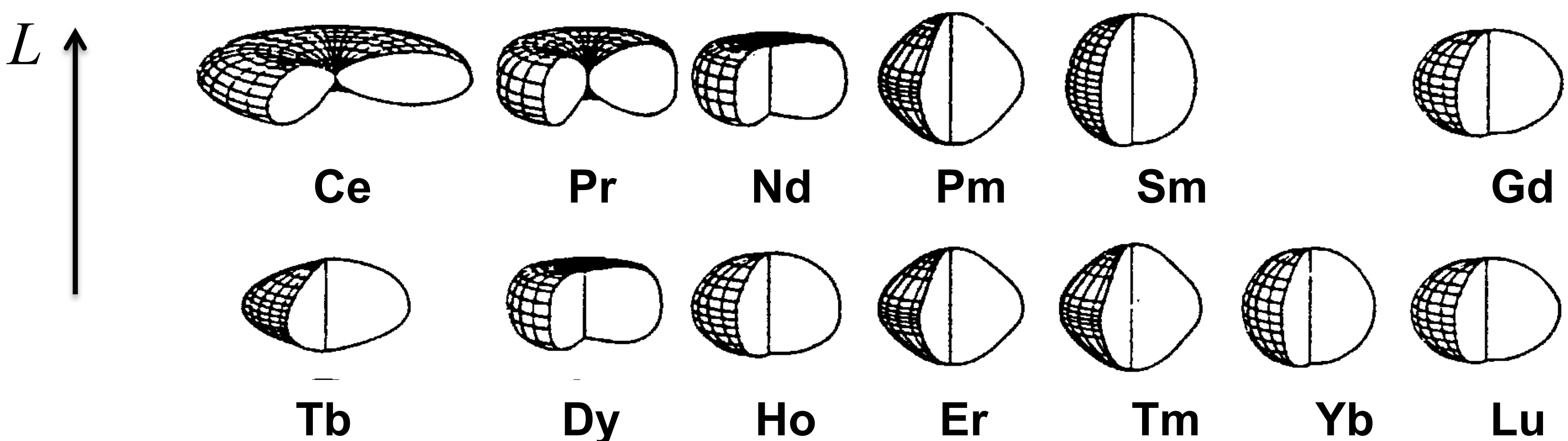


A. Sakuma

$$K_1 = -3J(J-1/2)\alpha_J \langle r^2 \rangle A_2^0$$

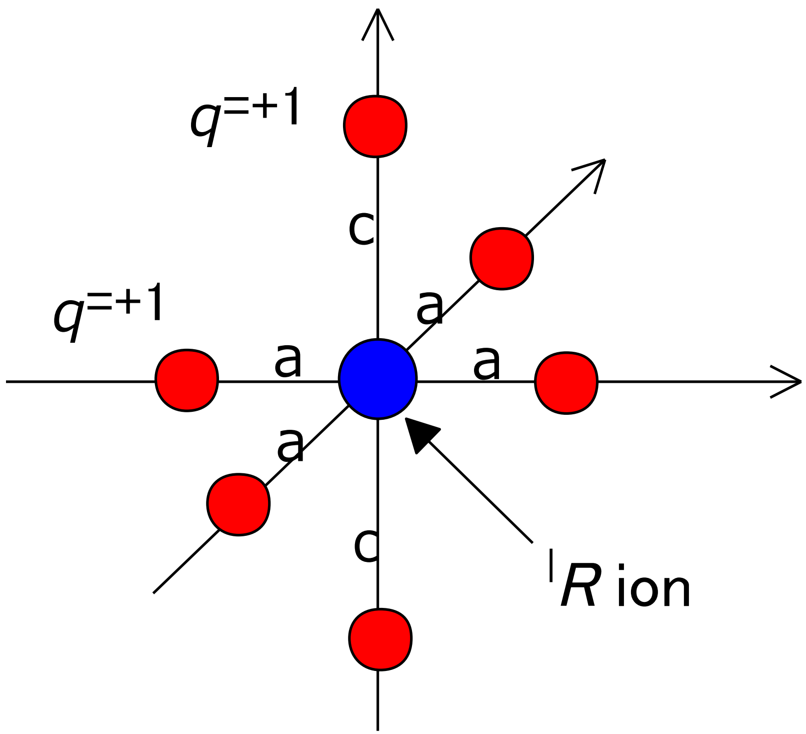


$$A_2^0(latt) = |e|\left(\frac{1}{a^3} - \frac{1}{c^3}\right)$$

$a < c \rightarrow \quad A_2^0 > 0 \qquad \therefore \alpha_J < 0$ (Nd, Dy etc.) $\Rightarrow K_1 > 0$

$a > c \rightarrow \quad A_2^0 < 0 \qquad \therefore \alpha_J > 0$ (Sm, Er etc.) $\Rightarrow K_1 > 0$

A. Sakuma

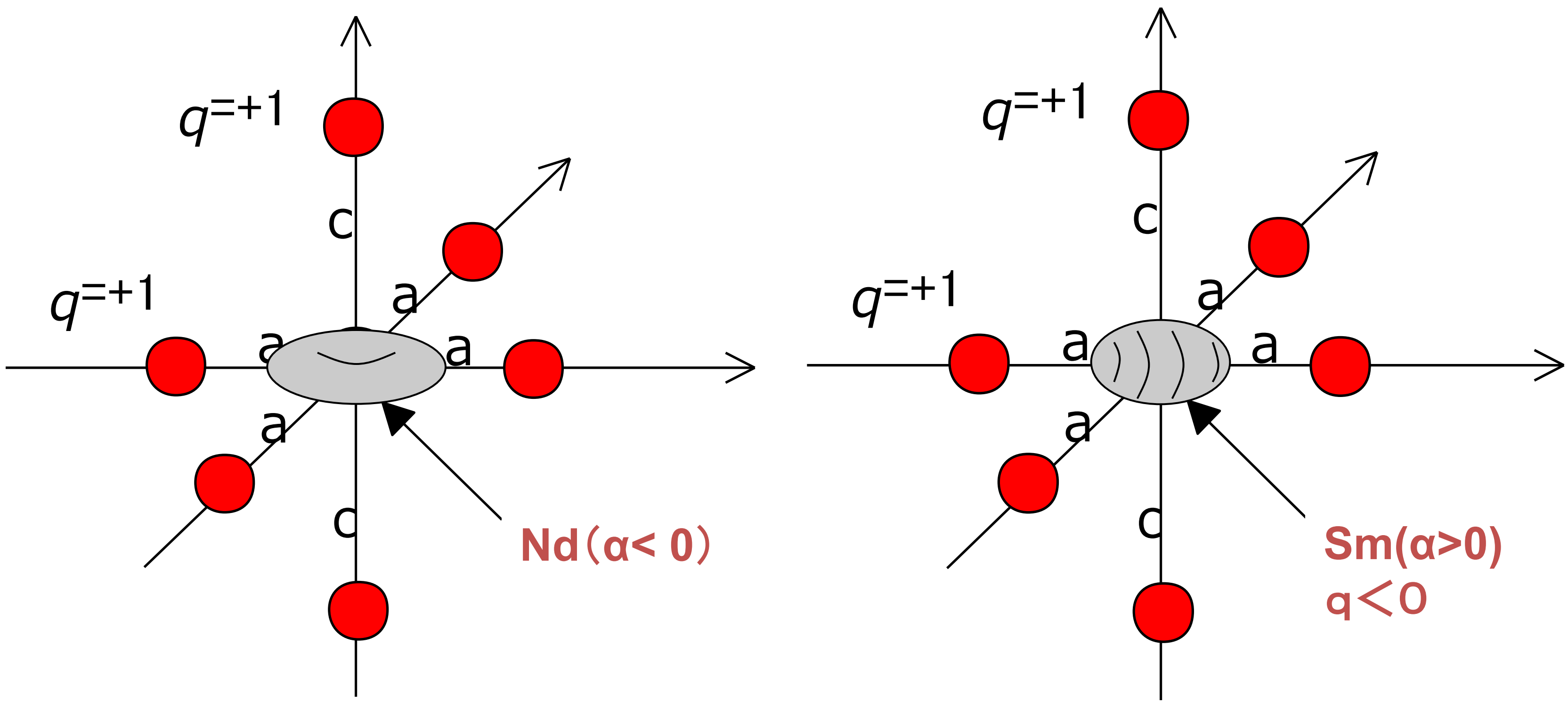


$$A_2^0(latt) = |e|\left(\frac{1}{a^3} - \frac{1}{c^3}\right) > 0$$

$a < c$

A. Sakuma

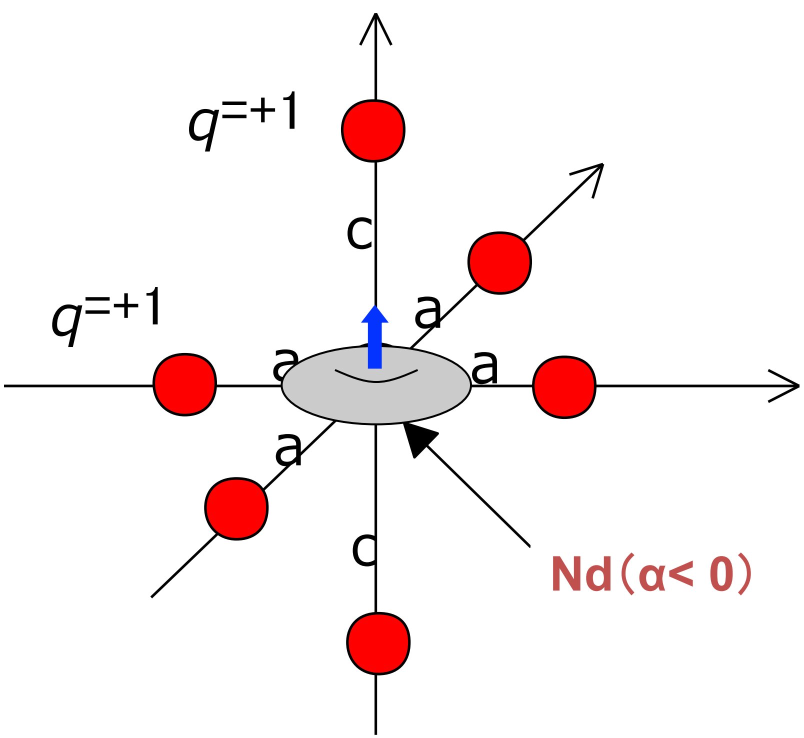


$K_1 > 0$

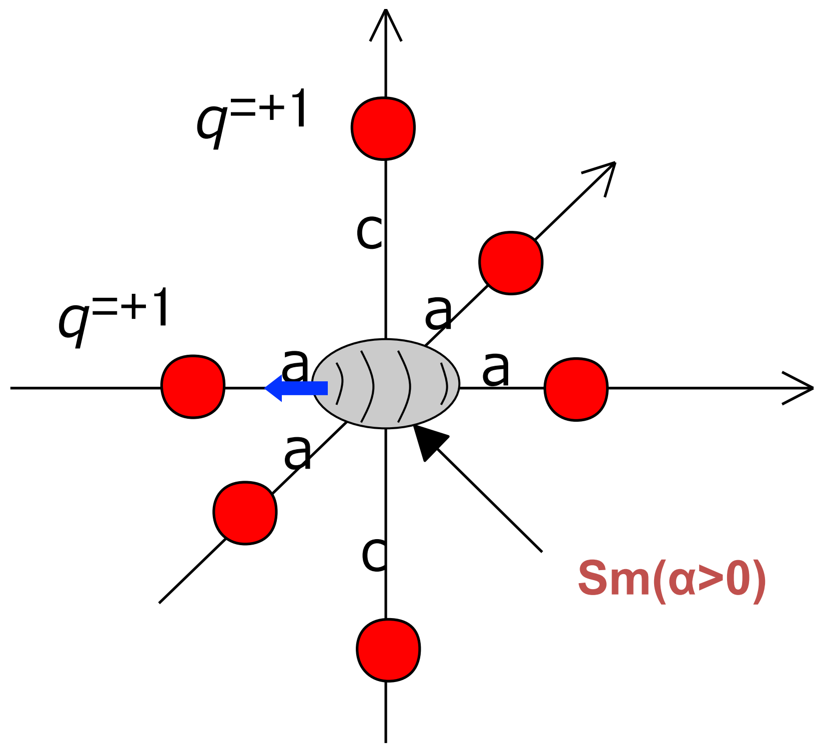


$K_1 < 0$

A. Sakuma

**CEF** $A_l^m$

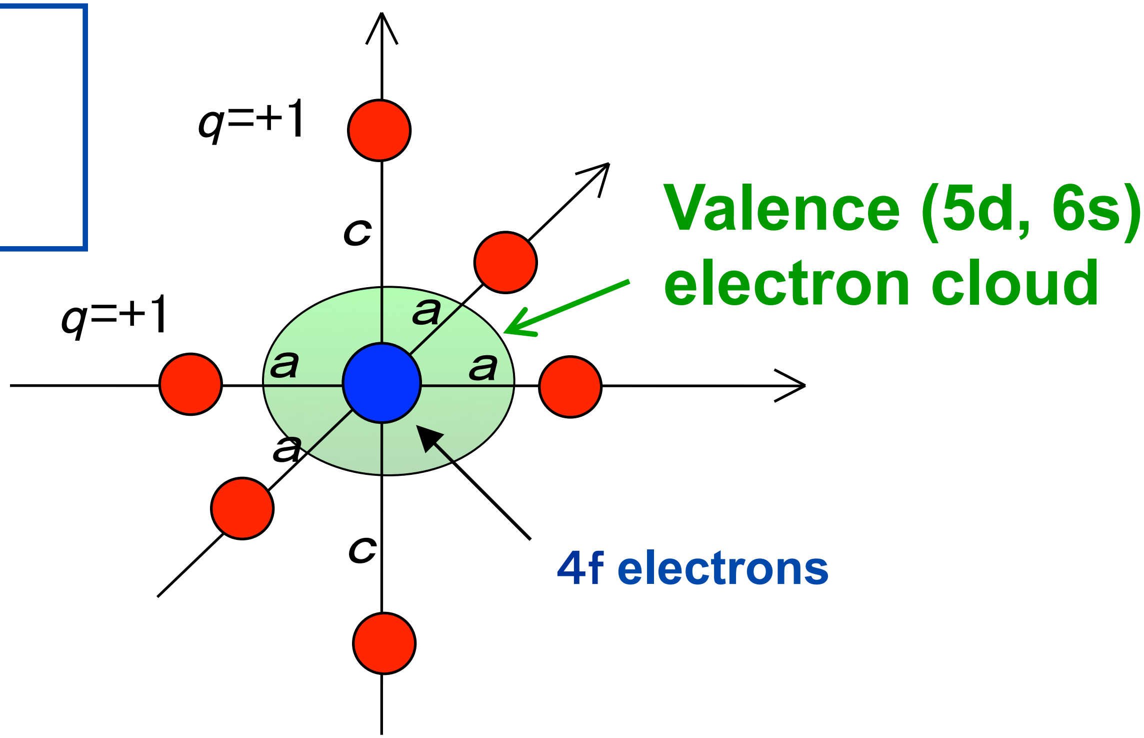


$$A_l^m = A_l^m(latt.) + A_l^m(val.)$$

**4f electron cloud**

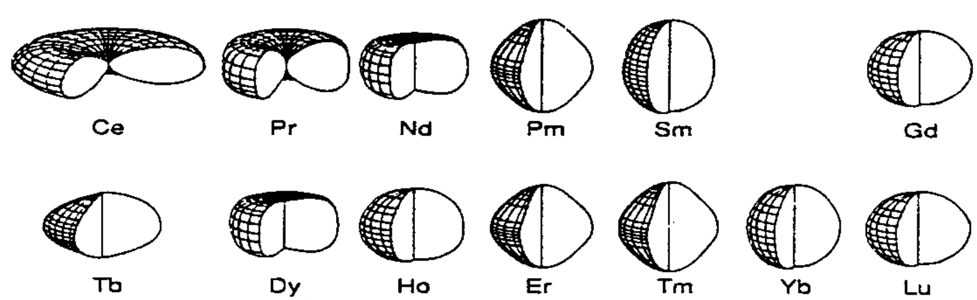


A. Sakuma

# Density Functional Theory

■ Reasonably good for *M* and *Tc* of 3*d* metals

*ex.*) exchange coupling $J_{ij}$ → Classical Heisenberg model

■ MCA energy

numerical problem for 3*d* metals

difficult to treat 4*f* electrons (LDA+U?, SIC? , ･･･)

# Slater–Pauling curve

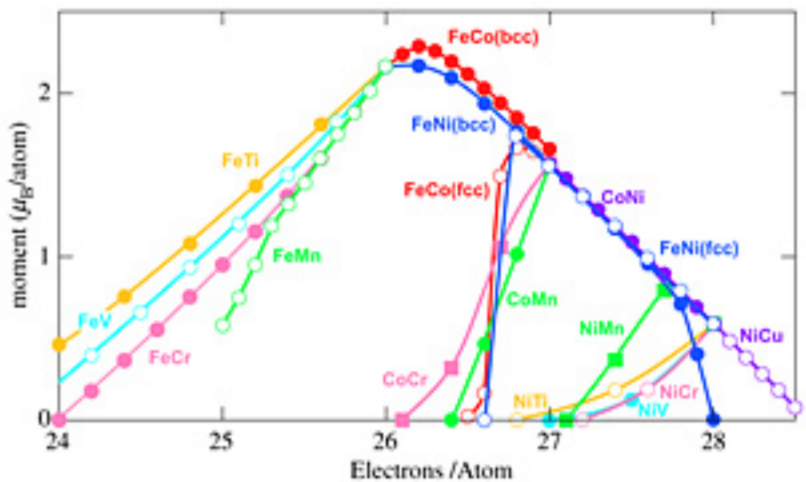


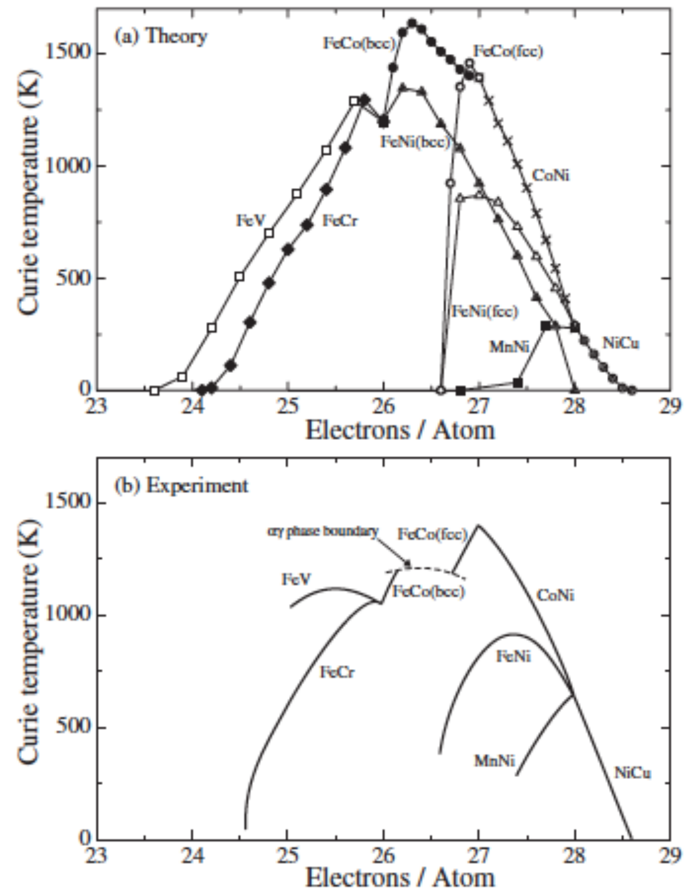


$$J_{ij} = \frac{1}{4\pi}\int^{E_F} d\epsilon\, \mathrm{Im}\mathrm{Tr}_L\{\Delta_i T_\uparrow^{ij}\Delta_j T_\downarrow^{ji}\}$$

Takahashi, Ogura and Akai,
J. Phys.: Cond. Mat. (2007)

# First-principles calculation of CEF parameters

Kohn–Sham equation

$$\left\{-\frac{\hbar^2}{2m}\Delta + v_{\text{eff}}(\mathbf{r})\right\}\psi_{\mathbf{k}j}(\mathbf{r}) = E_{\mathbf{k}j}\psi_{\mathbf{k}j}(\mathbf{r})$$

$$v_{\text{eff}}(\mathbf{r}) = \sum_{l=0}^{\infty}\sum_{m=-l}^{l} W_{lm}(r_R)\underline{Z_{lm}(\hat{\mathbf{r}}_R)}$$

real spherical harmonics

CEF parameters

$$A_{lm}\langle r_R^l\rangle = F_{lm}\langle W_{lm}\rangle = F_{lm}\int W_{lm}(r_R)\underline{\varphi^2(r_R)}\mathrm{d}r_R$$

4f atomic orbital

# Outline

- Coercivity and magnetocrystalline anisotropy
- Rare-earth magnets
- Standard theory
- An example: $NdFe_{11}TiN$
- Interface and magnetic reversal

# $RFe_{11}Ti$

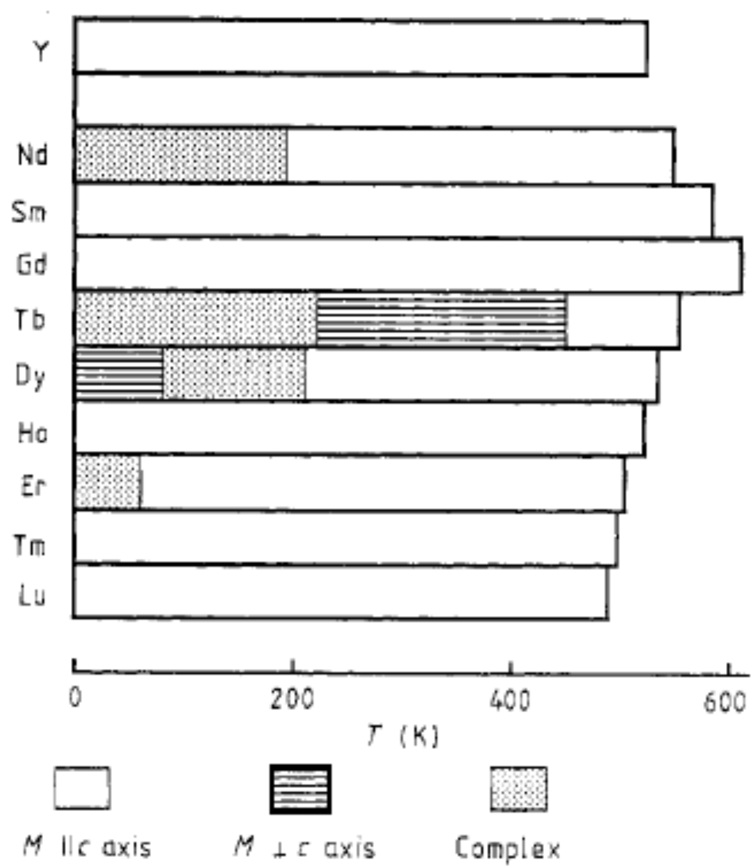


- $RFe_{12}$ is unstable
- $RFe_{12-x}M_x$ ($M$=Al,Ti,V,Cr,Mo,W,⋯ )
- Drastic change by N-doping

  ex.) uniaxial anisotropy in $NdFe_{11}TiN$

Hu et al., J. Phys: Cond.Mat. **1**, 755 (1989)

# $NdFe_{12}$ vs. $NdFe_{12}N$

| | $A_{20}\langle r^2\rangle$ |
|---|---|
| $NdFe_{12}$ | -83 K |
| $NdFe_{12}N$ | +413 K |

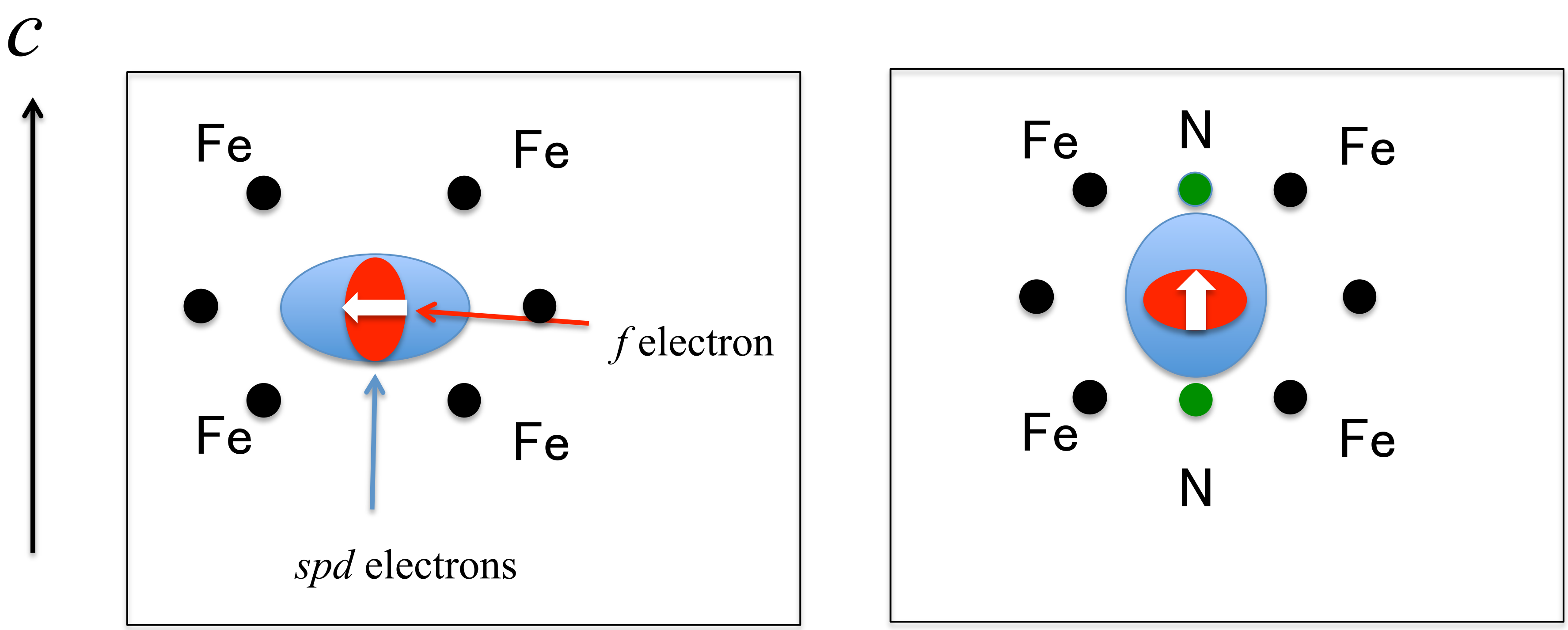

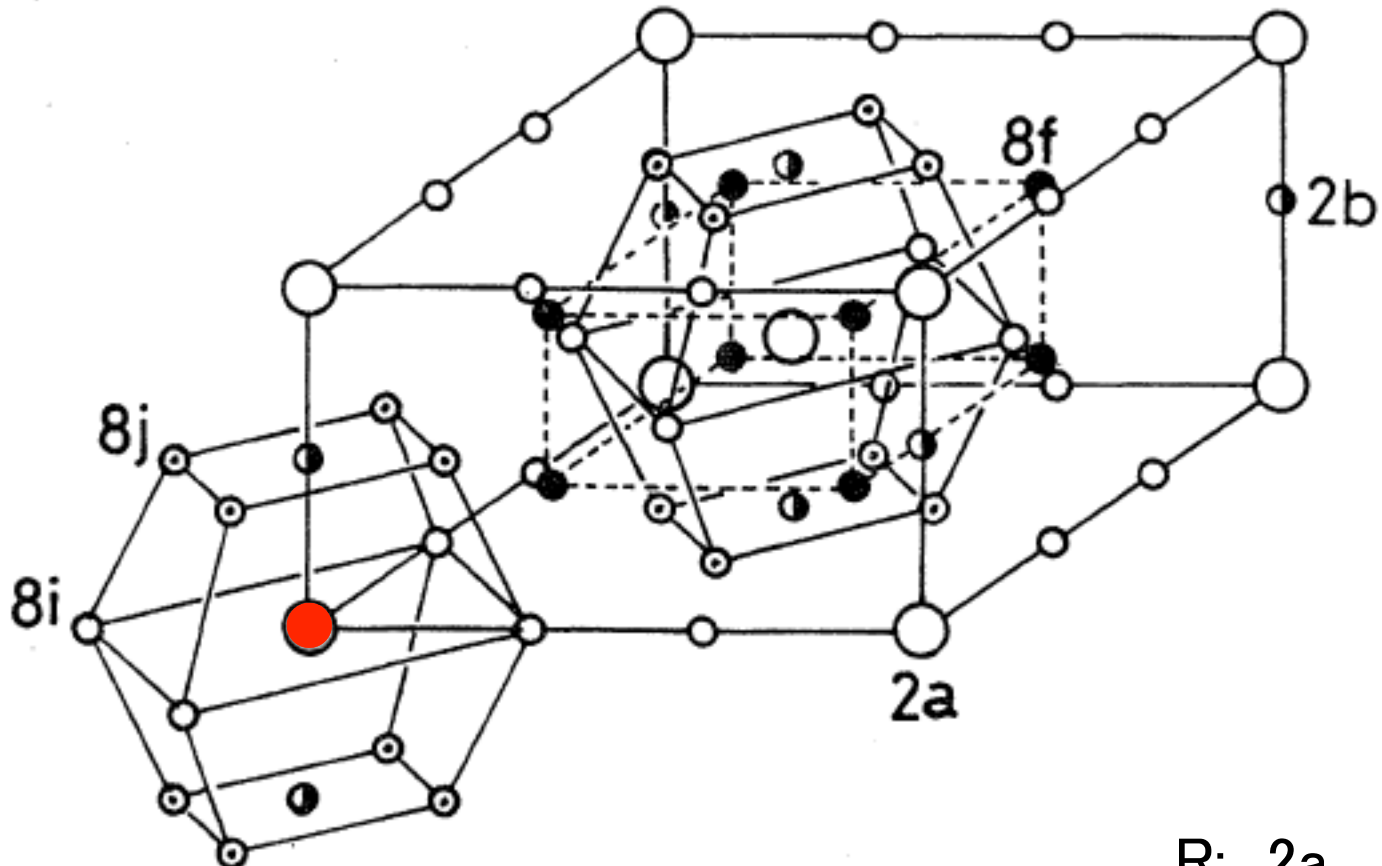


R: 2a
Fe: 8i, 8j, 8f
Ti: 8i
N: 2b

A.Sakuma, JPSJ **61**, 4119 (1992)

# $NdFe_{12}$ vs. $NdFe_{11}Ti$

| | $A_{20}\langle r^2 \rangle$ |
|---|---|
| $NdFe_{12}$ | -83 K |
| $NdFe_{11}Ti$ | +54 K |

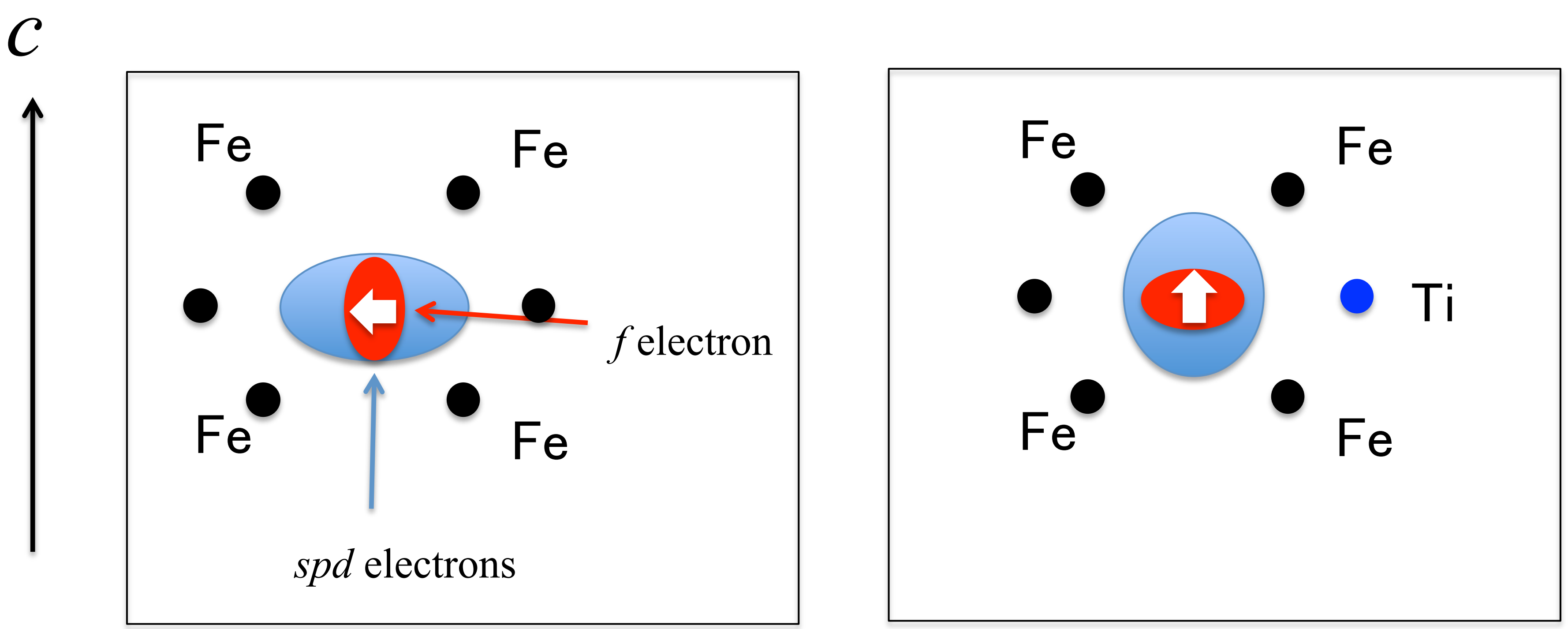

# Sintered magnet

(1) Grain boundary phase: microscopic structures and composition
(2) Magnetic properties at interfaces
(3) Relation between MCA and coercivity

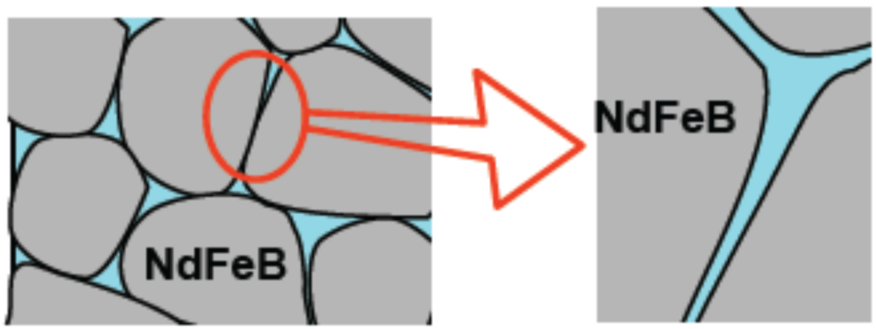


main phase : $Nd_2Fe_{14}B$
grain boundary phase : Fe–Cu–Nd amorphous, Nd oxides, ···

# $Nd_2Fe_{14}B$ surface

| | RE site | $Nd_2Fe_{14}B$ This work | $Nd_2Fe_{14}B$ LDA+ $U$ | $Dy_2Fe_{14}B$ |
|---|---|---|---|---|
| Surface | 4*f* | −908 | −413 | −954 |
| | 4*g* | −751 | −432 | −890 |
| Inside | 4*f* | 546 | 517 | 513 |
| | 4*g* | 777 | 291 | 585 |

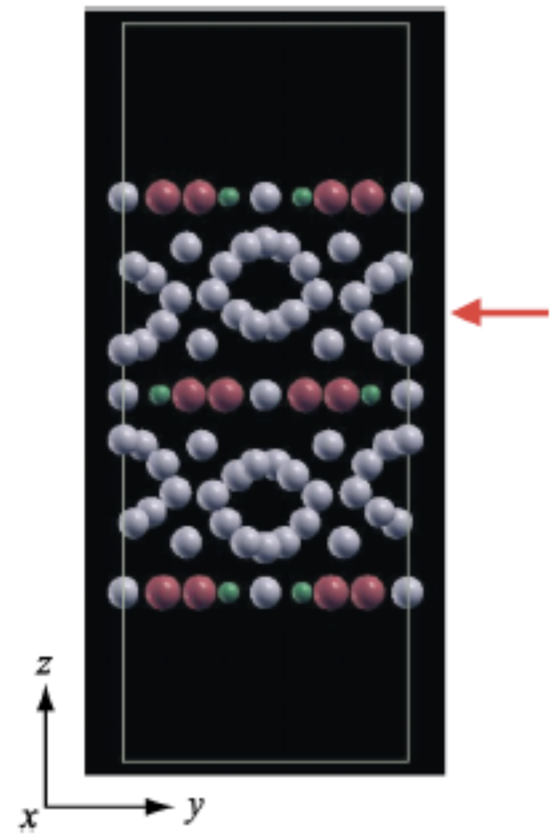


Moriya, Tsuchiura and Sakuma, J. Appl. Phys. 105, 07A740 (2009);
Tanaka et al., J. Appl. Phys. 109, 07A702 (2011)

# Micromagnetics

## Landau-Lifshitz-Gilbert (LLG) equation

$$\frac{\partial \boldsymbol{m}_i}{\partial t} = -\frac{|\gamma|}{1+\alpha^2}\left(\boldsymbol{m}_i \times \boldsymbol{H}_i^{\mathrm{eff}} + \frac{\alpha}{m_i}\left(\boldsymbol{m}_i \times \left(\boldsymbol{m}_i \times \boldsymbol{H}_i^{\mathrm{eff}}\right)\right)\right)$$

$$\boldsymbol{H}_i^{\mathrm{eff}} = \boldsymbol{H} + \boldsymbol{H}_i^{\mathrm{ex}} + \boldsymbol{H}_i^{\mathrm{a}}$$

$$\boldsymbol{H}_i^{\mathrm{ex}} = \sum_{j \neq i} \frac{J_j^{\mathrm{ex}}}{m} \frac{\boldsymbol{m}_j}{m_j}$$

$$\boldsymbol{H}_i^{\mathrm{a}} = \frac{2K_{\mathrm{u1}}}{m_j}\left(\frac{\boldsymbol{m}_j}{m_j} \cdot \boldsymbol{A}\right)\boldsymbol{A}$$

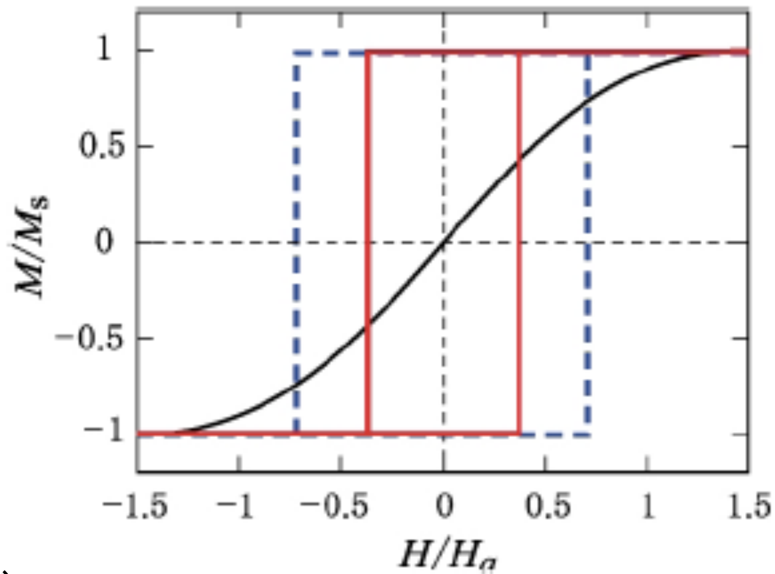


- Ab-inotio evaluation of parameters
- Spatial variation
- Large-scale simulation
  (coarse graining, massive-parallel calc.)

# Summary

- Coercivity and magnetocrystalline anisotropy
- Rare-earth magnets
- Standard theory
- An example: $NdFe_{11}TiN$
- Interface and magnetic reversal